



Flower-like hierarchical nickel microstructures: Facile synthesis, growth mechanism, and their magnetic properties

Huiyu Chen^{a,b,*}, Chunju Xu^c, Chuang Chen^{a,b}, Guizhe Zhao^{a,b}, Yaqing Liu^{a,b}

^a Research Center for Engineering Technology of Polymeric Composites of Shanxi Province, North University of China, Taiyuan 030051, People's Republic of China

^b College of Materials Science and Engineering, North University of China, Taiyuan 030051, People's Republic of China

^c School of Advanced Materials Science & Engineering (BK21), Sungkyunkwan University, Suwon 440746, Republic of Korea

ARTICLE INFO

Article history:

Received 18 July 2011

Received in revised form 5 March 2012

Accepted 18 April 2012

Available online 25 April 2012

Keywords:

A. Nanostructures

A. Magnetic materials

B. Chemical synthesis

B. Crystal growth

B. Magnetic properties

ABSTRACT

Flower-like hierarchical nickel microstructures were prepared by a facile chemical reduction method requiring 4 h at temperature of 85 °C without any template or external magnetic field. Nickel (II) sulfate hexahydrate was used as nickel source and hydrazine hydrate acted as the reducing agent. XRD study confirmed the highly crystalline with face-centered cubic (fcc) phase. SEM images revealed that the individual flower-like microstructures have an average diameter of 1–2 μm and are composed of sword-like nanopetals growing radially from the core of the spherical particles. HRTEM image and SAED pattern of the single petal show that the lattice spacing is 0.203 nm corresponding to the (1 1 1) plane of fcc nickel and the growth orientation is along [0 1 1] direction. A rational formation process of nickel microflowers was proposed. Magnetic hysteresis measurements revealed that the hierarchical nickel microstructures possess ferromagnetic behavior with an enhanced coercivity value of about 203.3 Oe.

© 2012 Elsevier Ltd. All rights reserved.

1. Introduction

In the past decades, the fabrication of micro-/nanomaterials with controllable shape and size has attracted increasing attention, because it is widely accepted that the intrinsic properties of these materials have a close relationship with their morphology, size, size distribution, and crystalline [1–3]. Recently, many efforts have been devoted to preparing hierarchical structures assembled by low-dimensional materials within nanoscale in that such three-dimensional (3D) assemblies are believed to exhibit novel properties different from their bulk counterparts and have potential applications in nanodevices [4,5]. Different driving mechanisms were proposed for the self-assembly of highly organized building blocks of metals and semiconductors [6–8]. As for the assembling magnetic nanocrystals into desired architectures, template or external magnetic fields are usually necessary [9,10]. However, the above methods still have some limitations. For example, the self-assembly route is considerably complicated and the usage of template inevitably adds to the complexity in the synthetic procedures. The magnetic-field-induced growth approach is inappropriate for industries due to the reliability on external magnetic field. Currently, it is still a big

challenge to develop simple and practical route for the direct preparation of magnetic hierarchical nanomaterials without any external assistance so as to fully exploit their peculiar properties and unique applications.

As an important ferromagnetic material, nickel has received much attention and has been the focus of intense research because of their diverse applications as catalyst, memory storage, magnetic fluid, and biomedical diagnosis [11–15]. Until now, nickel with different morphologies including nanoparticles [16], nanobelts [17], nanowires [18], nanochains [19], nanotubes [20], hollow spheres [21], and other 3D complex [22–24], has been synthesized by a variety of methods. Typically, nickel nanobelts were fabricated with the assistance of sodium dodecylbenzenesulfonate (SDBS) [17]. Nickel nanotubule array with 35 μm in length were obtained by electrodeposition in the pores of an alumina membrane [20]. Fu and coworkers prepared Ni dendritic nanostructures via a hydrothermal reduction approach in the presence of surfactant CTAB [25]. Nickel nanowires and nanoflowers were prepared by introducing a magnetic force into the reaction system [10]. Therefore, it is highly expected to synthesize controlled Ni hierarchical structures by a facile and practical method such as the variation of reaction time, concentrations, and so forth, without employing the external assistance including template or magnetic force.

In this work, we reported a simple chemical reduction method to the fabrication of flower-like hierarchical nickel microstructures by reducing nickel sulfate hexahydrate with hydrazine in the absence of any template or external magnetic field. The ligand

* Corresponding authors at: College of Materials Science and Engineering, North University of China, Taiyuan 030051, People's Republic of China.

Tel.: +86 351 3557256; fax: +86 351 3557256.

E-mail addresses: hychen09@sina.com (H. Chen), zfflyq98@163.com (Y. Liu).

agent of ethylenediamine played a key role for the formation of nickel micro-flowers, and two-stage grow process was rational proposed for the formation mechanism on the basis of a series of controlled experiments. Magnetic measurements demonstrate that as-synthesized fcc phase nickel with a hierarchical microstructure show ferromagnetic behavior with an enhanced coercivity compared to bulk counterpart.

2. Experimental

2.1. Materials

All chemical reagents were purchased from Sigma–Aldrich and used without further purification. Nickel (II) sulfate hexahydrate, ethylenediamine, sodium hydroxide, and hydrazine hydrate were used as received.

2.2. Synthesis of flower-like nickel microstructures

In a typical synthesis, 12 g of NaOH was dissolved in deionized water (20 mL) by intensively magnetic stirring, then 1 mL of $\text{NiSO}_4 \cdot 6\text{H}_2\text{O}$ (0.1 mol/L) solution and 0.35 mL of ethylenediamine (EDA) were introduced. After the mixture was continuously stirred for 20 min, 0.25 mL of $\text{N}_2\text{H}_4 \cdot \text{H}_2\text{O}$ (hydrated hydrazine 30%) was added dropwise to the above solution. The obtained precursor was stirred for another 10 min, and then transferred to a 50 mL glass bottle followed by heating to 85 °C and holding for 4 h. After the heat treatment, the black fluffy product floating on the solution was collected by magnetic bar, rinsed with distilled water and absolute ethanol several times to remove any alkaline and byproduct that remained in the final products, and then finally dried in air at 40 °C for 3 h. Controlled experiments were carried out by changing the reaction time and dosage of ethylenediamine, respectively, while kept other synthetic parameters and procedure the same as those of typical reaction.

2.3. Characterizations

The phase purity of the Ni product was examined by X-ray powder diffraction (XRD) with a Bruker D8 focus diffractometer at a voltage of 40 kV and a current of 40 mA with a $\text{Cu K}\alpha$ radiation ($\lambda = 0.15406$ nm), employing a scanning rate of $4^\circ/\text{m}$ in the 2θ range from 30° to 100° . Field emission scanning electron microscopy (FESEM) images were taken on a JEOL JSM-6700F scanning electron microscope. The transmission electron microscopy (TEM and HRTEM) images and the corresponding selected area electron diffraction (SAED) patterns were captured on a JEOL JEM-2100F transmission electron microscope at an acceleration voltage of 200 kV. The magnetic property of the flower-like Ni sample was measured in a vibrating sample magnetometer (VSM)

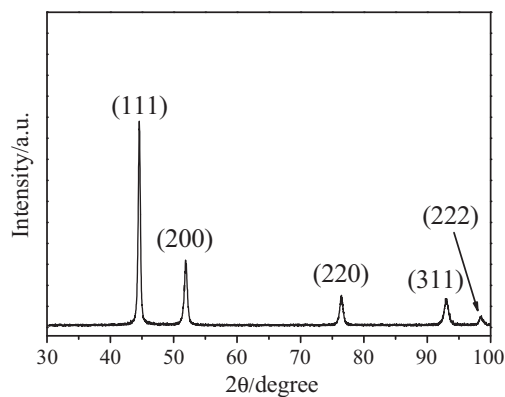


Fig. 1. XRD pattern of the obtained flower-like nickel microstructures.

(Lakeshore 7407, USA). Magnetization curve was recorded at room temperature by first saturating the sample powder in a field of 5000 Oe, and then the saturation magnetization (M_s), the remanent magnetization (M_r), and the coercivity (H_c) were determined for the sample.

3. Results and discussion

The phase structure and purity of the as-obtained Ni sample was examined by XRD. As the XRD pattern shown in Fig. 1 that five characteristic peaks can be indexed as the (1 1 1), (2 0 0), (2 2 0), (3 1 1), and (2 2 2) planes of the face-centered cubic (fcc) phase Ni with lattice constant $a = 3.522$ Å, which is in good agreement with the reported data (JCPDS No. 04–0850, $a = 3.524$ Å). It was worth noting that the relative diffraction peak intensity ratio of the {1 1 1} facets to {2 0 0} facets for the sample (3.33) is higher than that for the conventional value (1.92). The significantly intensified {1 1 1} diffraction peak implies the orientation of the {1 1 1} crystallographic plane. No characteristic peaks due to the impurities such as nickel oxides or hydroxides were detected, which indicated that metallic Ni product was obtained under the current synthesis conditions.

The morphology of nickel product was investigated by SEM and a typical SEM image with panoramic view was displayed in Fig. 2a, from which we could clearly observe that the sample possessed uniform flower-like shape with an average diameter of 2 μm. Further observation from high magnification SEM image (Fig. 2b) demonstrated that the nickel micro-flowers consisted of a spherical core attached with many sword-like petals. These petals grew radially from the spherical core with diameters of 150–250 nm at the root and lengths of 200–400 nm from the root to the tip.

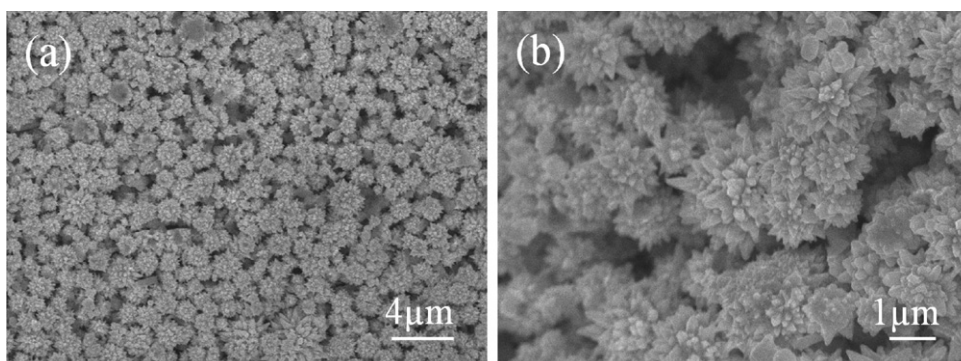


Fig. 2. SEM images of the obtained flower-like nickel microstructures with (a) panoramic view and (b) high magnification view.

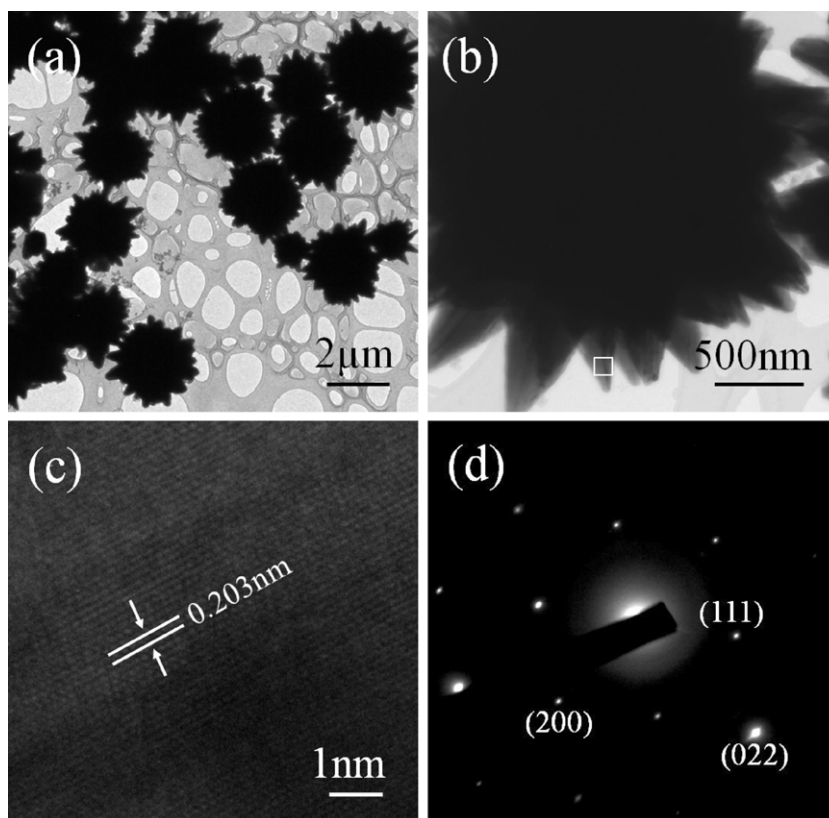


Fig. 3. TEM images of (a) nickel micro-flowers with panoramic view and (b) individual sample with enlarged view.

Fig. 3a shows a representative TEM image with low magnification view. It could be observed more clearly that the nickel micro-flowers have a quasi spherical core with plenty of sword-like petals protruding out of the core surface and radiating to various directions. The average size of individual micro-flower is about 2 μm , consistent with the observation from SEM images. Interestingly, the flower-like structure cannot be destroyed into discrete petals even under a long period of time of ultrasonication, indicating that the complex architectures are actually integrated and not made up of loosely aggregated nanopetals through magnetic dipole interactions. The microstructure of the petals was studied by high-resolution TEM (HRTEM). Fig. 3b is an enlarged TEM image of a partial micro-flower with the petals observed clearly. The corresponding HRTEM image (Fig. 3c) was taken from the position enclosed in a white box in Fig. 3b. The regular spacing of the observed lattice plane was ca. 0.203 nm, which was consistent with the separation of $\{1\ 1\ 1\}$ planes of fcc nickel. Fig. 3d is the corresponding selected area electron diffraction (SAED) pattern, which exhibits a regular and clear diffraction spot array. Therefore, a single crystal nature of the petal could be concluded. Combined the HRTEM and SAED analysis, it is evident that the sword-like petal of flower-like nickel microstructure grows along $[0\ 1\ 1]$ direction and agrees well with the XRD result.

In order to investigate the formation process of such novel flower-like nickel microstructures, time-dependent experiments were carried out while other synthetic parameters were kept unchanged. The samples were collected at different time intervals as the SEM images shown in Fig. 4. At the early stage with reaction time of only 30 min, the nickel product was dominated by particles with diameters ranging from 0.3 to 0.6 μm (Fig. 4a). The sample collected 1.5 h later was composed of microparticles with fine hierarchical nanoarchitectures and the average size was about 1.5 μm (Fig. 4b). Meanwhile, particles with diameter of ca. 0.5 μm were also coexisted. If we continued to prolong the time to 3 h, the

amount of microparticles with fine hierarchical nanoarchitectures were greatly increased at the expense of smaller particles. The petals were initially developed at this stage as the SEM image was shown in Fig. 4c. The size of nickel microparticles with fine hierarchical nanoarchitectures would grow gradually. Eventually, nickel micro-flowers composed entirely of nanopetals were formed (Figs. 2 and 4d) when the time was increased to 4 h. Similar hierarchical microstructures were previously prepared for several kinds of metals. The formation mechanism involved the surfactant assistance, or included that smaller nanoparticles self-assembled into complicated microstructures [26–28]. However, in our case, the whole evolution process is consistent with the previous reports of so called two-stage growth process [29–31], during which the time factor is the most important one and four types of samples could be obtained with different time intervals: (1) particles with size ranging from a few hundred nanometers to micrometer scale; (2) smaller particles and microparticle with fine hierarchical nanoarchitectures; (3) microparticle with fine hierarchical nanoarchitectures; and (4) a spherical hierarchical nanoarchitectures with high yield. This growth mechanism included a fast nucleation of primary particles followed by a slow aggregation and crystallization of primary particles. In our work, Ni^{2+} was first coordinated with ethylenediamine (EDA) to form a relative stable complex $[\text{Ni}(\text{EDA})_3]^{2+}$, then this complex was reduced to form nuclei and quickly grew into the primary particles. In the subsequent growth stage, the primary particles aggregated into microspheres that became the core of hierarchical nanoarchitected microparticles. At the same time, EDA was released and acted as surfactant to assist formation of finally flower-like nickel microstructures.

As discussed above, EDA acted not only as a ligand to produce $[\text{Ni}(\text{EDA})_3]^{2+}$ but also as a surfactant when it was released. We believe EDA plays important role in the formation of hierarchical nickel micro-flowers and Fig. 5 shows the SEM images of nickel

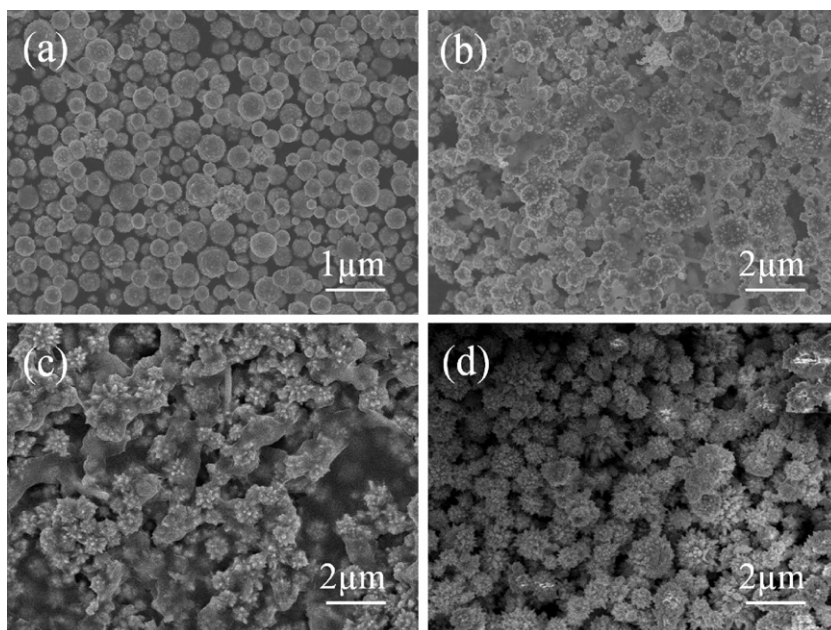


Fig. 4. SEM images of nickel samples synthesized with reaction time of (a) 30 min, (b) 1.5 h, (c) 3 h, and (d) 4 h.

products prepared with various amount of EDA. The sample was dominated by microparticles with mean size of ca. 1 μm when no EDA was employed (Fig. 5a). Irregular microparticles coexisted with some undeveloped flower-like structures in the final product when 0.1 mL was introduced to the synthetic system (Fig. 5b). It was obvious that the quantity of EDA is not enough for the current synthesis of nickel micro-flowers. However, if we further increased EDA to 0.35 mL or more, separate flower-like hierarchical microstructures were obtained as the dominant product. Especially, when EDA with amount of 1 mL was added, some Ni flowers possess fewer petals compared to those obtained with 0.35 mL EDA in the typical synthesis, while such assembled petals have large diameters and longer length (Fig. 5c). The formation of

$[\text{Ni}(\text{EDA})_3]^{2+}$ can decrease the free Ni^{2+} concentration in the solution and result in the slow generation of Ni nanoparticles. The reaction rate can therefore be tuned, which can regulate the kinetics of nucleation and growth of the products and further efficiently control the shape and structures of the final product. On the other hand, the EDA released from the complex $[\text{Ni}(\text{EDA})_3]^{2+}$ after the reduction reaction was considered to kinetically control the growth rates of different crystallographic facets of Ni micro-flowers through preferentially adsorbing and desorbing on these facets.

The dosage of reducing agent was another important factor to influence the final morphology of nickel sample. An experiment was carried out with larger amount (2 mL) of hydrated hydrazine

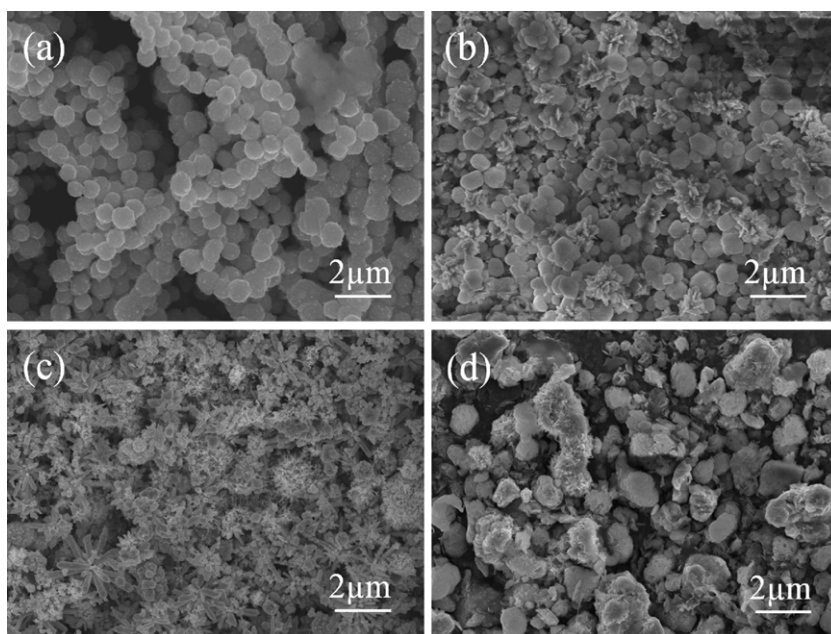


Fig. 5. SEM images of nickel samples prepared with (a) 0 mL, (b) 0.1 mL, (c) 1 mL ethylenediamine, and (d) SEM image of nickel sample synthesized with 2 mL hydrated hydrazine and 0.35 mL ethylenediamine.

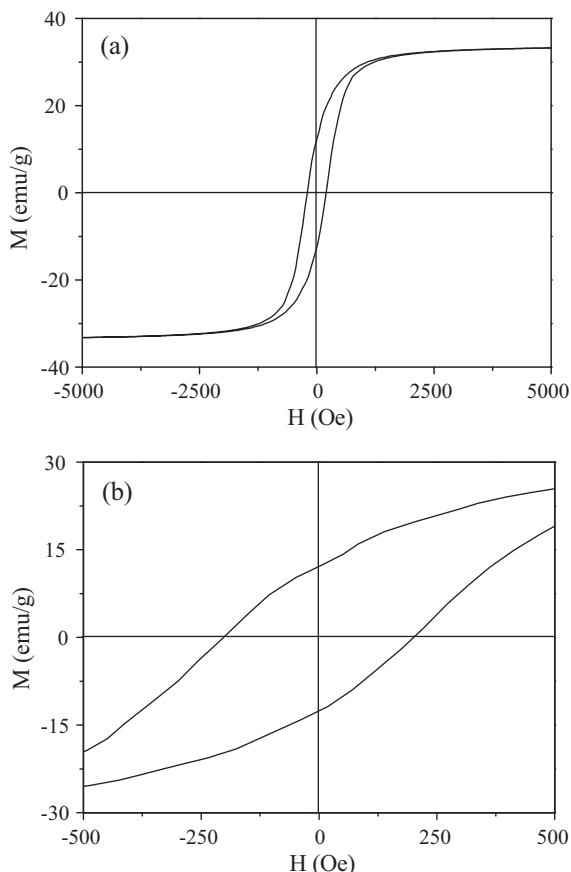


Fig. 6. (a) Magnetic hysteresis loop of the flower-like hierarchical nickel microstructures measured at room temperature and (b) the hysteresis loop at low field.

for a comparison. We could clearly observe from Fig. 5d that the sample was dominated by irregular microparticles with very broad size distribution. Some micropatches were also produced. The reaction rate was so high with 2 mL of $N_2H_4 \cdot H_2O$ used that the nucleation step could not be effectively separated from the subsequent growth stage and resulted in the formation of irregular microparticles. Therefore, minute amount of hydrated hydrazine is beneficial to obtain hierarchical nickel microflowers in the current synthesis.

Magnetic measurement of the as-prepared flower-like nickel microstructures were conducted at room temperature in an applied magnetic field sweeping from -5000 to 5000 Oe, and the hysteresis loop is shown in Fig. 6a. The sample displays hysteresis behavior, revealing that the nickel microstructures are ferromagnetic. The saturation magnetization (M_s) value is ca. 33.5 emu/g, which is lower than that of the bulk nickel (55 emu/g) [32]. The reduced M_s value may be owing to a very thin layer of NiO, which cannot be clearly detected by diffraction methods, formed on the surface. Tracy et al. [33] reported the growth of thin NiO shells on nickel nanoparticles and confirmed that the M_s values were decreased due to the NiO formation, and the detailed M_s values were dependent on the Ni core size and NiO shell thickness. It was found from the magnified hysteresis loop at low applied field (Fig. 6b) that the remanent magnetization (M_r) and the coercivity (H_c) for the sample are 12.2 emu/g and 203.3 Oe, respectively. Compared to the coercivity value of bulk Ni (ca. 0.7 Oe) [17] and that of hollow nickel submicrometer spheres (ca. 32.3 Oe) [34], hollow Ni nanospheres (102 Oe) [21], or dandelion-like Ni nanostructures (ca. 130 Oe) [35] at room temperature, the flower-like Ni microstructures exhibit an enhanced value.

However, this value is lower than that of one-dimensional Ni nanorods (ca. 332 Oe) [36] or nanobelts (ca. 640 Oe) [17] with high anisotropy. The magnetic properties of nanomaterials have been widely accepted to be highly dependent on the sample morphology, size, crystallinity, magnetization direction, and so on [24]. The nickel micro-flowers prepared in the present work possess hierarchical structure leading to the surface/volume ratio and enhanced shape anisotropy. Hence, higher coercivity value was observed compared to that of bulk nickel and hollow nickel spheres.

4. Conclusions

In summary, hierarchical nickel micro-flowers were synthesized at a relatively low temperature of 85 °C without using any temperature or external magnetic field. The individual flower-like microstructures have an average diameter of $1\text{--}2$ μm and are composed of sword-like nanopetals growing radially from the core of the spherical particles. The formation mechanism of such nickel micro-flowers was governed by a two-stage growth process. It was found that synthetic parameters such as reaction time, dosage of ligand ethylenediamine and hydrazine hydrate were crucial to the formation of flower-like nickel. The magnetic measurement indicated that the as-obtained product had a ferromagnetic behavior with a significantly enhanced coercivity value compared to that of bulk nickel. The present facile method can be extended to fabricate other micro-/nanomaterials with similar hierarchical structures.

Acknowledgment

The authors gratefully acknowledge the financial support from High-level Scientific Research Foundation for the Introduction of Talent through North University of China.

References

- [1] Y.N. Xia, P.D. Yang, Y.G. Sun, Y.Y. Wu, B. Mayers, B. Gates, Y.D. Yin, F. Kim, H.Q. Yan, *Adv. Mater.* 15 (2003) 353.
- [2] K. Nagaveni, A. Gayen, G.N. Subbanna, M.S. Hegde, *J. Mater. Chem.* 12 (2002) 3147.
- [3] Y.G. Sun, Y.N. Xia, *Science* 298 (2002) 2176.
- [4] W. Alejandro, A. Onur, P.V. Braun, *J. Am. Chem. Soc.* 127 (2005) 16356.
- [5] V. Lionel, S. Conny, S.M. Butorin, *Adv. Mater.* 17 (2005) 2320.
- [6] G. Kaltenpoth, M. Himmelhaus, L. Slansky, F. Caruso, M. Grunze, *Adv. Mater.* 15 (2003) 1113.
- [7] J. Hu, L. Ren, Y. Guo, H. Liang, A. Cao, L. Wan, C. Bai, *Angew. Chem. Int. Ed.* 44 (2005) 1269.
- [8] P. Gao, Z. Wang, *J. Am. Chem. Soc.* 125 (2003) 11299.
- [9] L. Manna, E.C. Scher, A.P. Alivisatos, *J. Am. Chem. Soc.* 122 (2000) 12700.
- [10] F.L. Jia, L.Z. Zhang, X.Y. Shang, Y. Yang, *Adv. Mater.* 20 (2008) 1050.
- [11] J.G. Park, W.S. Nam, S.H. Seo, Y.G. Kim, Y.H. Oh, G.S. Lee, U.G. Paik, *Nano Lett.* 9 (2009) 1713.
- [12] F.Y. Cheng, J. Chen, X.L. Gou, *Adv. Mater.* 18 (2006) 2561.
- [13] R.Y. Zhang, L. Amlani, J. Baker, J. Tresek, R.K. Tsui, *Nano Lett.* 3 (2003) 731.
- [14] L. Sun, P.C. Searson, C.L. Chien, *Appl. Phys. Lett.* 79 (2001) 4429.
- [15] S. Pignard, G. Goglio, A. Radulescu, L. Piraux, S. Dubois, A. Declémy, J.L. Duvail, *J. Appl. Phys.* 87 (2000) 824.
- [16] Y. Hou, H. Kondoh, T. Ohta, S. Gao, *Appl. Surf. Sci.* 241 (2005) 218.
- [17] Z.P. Liu, S. Li, Y. Yang, S. Peng, Z.K. Hu, Y.T. Qian, *Adv. Mater.* 15 (2003) 1946.
- [18] X.R. Li, Y.Q. Wang, G.J. Song, Z. Peng, Y.M. Yu, X.L. She, J.J. Li, *Nanoscale Res. Lett.* 4 (2009) 1015.
- [19] C.M. Liu, L. Guo, R.M. Wang, Y. Deng, H.B. Xu, S.H. Yang, *Chem. Commun.* 25 (2004) 2726.
- [20] J.C. Bao, C.Y. Tie, Z. Xu, Q.F. Zhou, D. Shen, Q. Ma, *Adv. Mater.* 13 (2001) 1631.
- [21] Q. Liu, H.J. Liu, M. Han, J.M. Zhu, Y.Y. Liang, Z. Xu, Y. Song, *Adv. Mater.* 17 (2005) 1995.
- [22] J.G. Guan, L.J. Lin, L.L. Xu, Z.G. Sun, Y. Zhang, *CrystEngComm* 13 (2011) 2636.
- [23] S. Senapati, S.K. Srivastava, S.B. Singh, K. Biswas, *Cryst. Growth Des.* 10 (2010) 4068.
- [24] L.P. Zhu, G.H. Liao, W.D. Zhang, Y. Yang, L.L. Wang, H.Y. Xie, *Eur. J. Inorg. Chem.* 8 (2010) 1283.
- [25] X.M. Liu, S.Y. Fu, *J. Cryst. Growth* 306 (2007) 428.
- [26] B. Zhang, P. Xu, X.M. Xie, H. Wei, Z.P. Li, N.H. Mack, X.J. Han, H.X. Xu, H.L. Wang, *J. Mater. Chem.* 21 (2011) 2495.

- [27] C. Wang, X.J. Han, X.L. Zhang, S.R. Hu, T. Zhang, J.Y. Wang, Y.C. Du, X.H. Wang, P. Xu, J. Phys. Chem. C 114 (2010) 14826.
- [28] C. Wang, X.J. Han, P. Xu, J.Y. Wang, Y.C. Du, X.H. Wang, W. Qin, T. Zhang, J. Phys. Chem. C 114 (2010) 3196.
- [29] Y. Cheng, Y.S. Wang, Y.H. Zheng, Y. Qin, J. Phys. Chem. B 109 (2005) 11548.
- [30] R.L. Penn, J. Phys. Chem. B 108 (2004) 12707.
- [31] L.P. Zhu, W.D. Zhang, H.M. Xiao, Y. Yang, S.Y. Fu, J. Phys. Chem. C 112 (2008) 10073.
- [32] J.H. Hwang, V.P. Dravid, M.H. Teng, J.J. Host, B.R. Elliott, D.L. Johnson, T.O. Mason, J. Mater. Res. 12 (1997) 1076.
- [33] A.C. Johnston-Peck, J.W. Wang, J.B. Tracy, ACS Nano 3 (2009) 1077.
- [34] J.C. Bao, Y.Y. Liang, Z. Xu, L. Si, Adv. Mater. 15 (2003) 1832.
- [35] J.T. Tian, C.H. Gong, L.G. Yu, Z.S. Wu, Z.J. Zhang, Chin. Chem. Lett. 19 (2008) 1123.
- [36] X.M. Ni, X.B. Su, Z.P. Yang, H.G. Zheng, J. Cryst. Growth 252 (2003) 612.